



# *In silico* design criteria for high blocking barrier uranium (III) SIMs†

 Sourav Dey  and Gopalan Rajaraman \*

 Cite this: *Chem. Commun.*, 2022, 58, 6817

 Received 7th March 2022,  
Accepted 12th May 2022

DOI: 10.1039/d2cc01356h

[rsc.li/chemcomm](https://rsc.li/chemcomm)

**A combination of DFT and *ab initio* CASSCF/PT2 calculations on U(III) fictitious models and numerous reported X-ray structures unveils several geometries from coordination number 1 to 12 that can be targeted to design potential U(III) SIMs with attractive barrier heights. Among the geometries studied, the T-shaped and capped pentagonal antiprism geometries yield values exceeding 1500 cm<sup>-1</sup> – a value that is elusive for any uranium SIMs.**

Single-molecule magnets (SMMs) are fascinating for chemists due to their potential applications in memory storage devices, qubits *etc.*<sup>1</sup> The performance of an SMM is determined by the blocking barrier of magnetisation reversal ( $U_{\text{eff}}$ ) and blocking temperature ( $T_{\text{B}}$ ), with the latter being more crucial for realising the potential applications listed.<sup>2,3</sup> However, experimentally, the extraction of  $U_{\text{eff}}$  is straightforward, but there are multiple ways to obtain  $T_{\text{B}}$  values.<sup>2</sup> A breakthrough in lanthanide SMMs has been achieved in pseudo two coordinate “Dysprocenium” complexes where  $T_{\text{B}}$  values beyond the liquid nitrogen temperature were achieved.<sup>4</sup> A recent theoretical study suggests that  $T_{\text{B}}$  is proportionate with the crystal field (CF) splitting in “Dysprocenium” complexes.<sup>5</sup> In lanthanide SMMs, the CF splitting can be considered the highest possible  $U_{\text{eff}}$ , though a direct correlation of  $U_{\text{eff}}$  and  $T_{\text{B}}$  is possible only in a select class of SIMs. The CF splitting of the lanthanide complexes has reached its axial limit, and therefore, further enhancement of  $T_{\text{B}}$  in mononuclear lanthanide complexes is a challenging task. Furthermore, Yin and co-workers recently suggested a long QTM relaxation time as an additional figure of merit for high-performance Dy(III) SIMs.<sup>3</sup>

The diffuse 5f orbitals of actinides offer large CF splitting since they are less deeply buried compared to 4f orbitals of lanthanides.<sup>1a</sup> Despite having improved properties for high-performance SMMs,

significant progress has not been made on actinide-based SMMs due to radioactivity and complexity in their electronic structures. Most of the reported actinide-based SIMs (single-ion magnets) are found to contain U(III) ions with a pyrazolyl borate ligand.<sup>6</sup> Although the role of coordination number and geometry in magnetic anisotropy has been studied in detail for lanthanide SMMs, the same has not been established for actinide SMMs.<sup>7</sup> The magnetic anisotropy in actinides is likely to be influenced by: (i) the ligand field around the metal ion,<sup>7a</sup> and (ii) the symmetry/pseudo symmetry of the first coordination sphere around the metal ion.<sup>7b</sup> For lanthanides, several *in silico* models with various coordination numbers are available, demonstrating which metal ion and ligand combination yields the best SMMs,<sup>7b,8</sup> and this design principle has seeded the growth of lanthanide-based SMMs. There are no such design principles available for actinides to date.

Keeping this in mind, here we have performed *ab initio* CAS(3,7)SCF/CASPT2/RASSI-SO/SINGLE\_ANISO calculations on seventeen U(III) models with the molecular formula of  $[\text{U}(\text{OH})_n(\text{H}_2\text{O})_m]^{+(0-2)}$  ( $n = 1-3$ ,  $m = 0-10$ ) with the coordination number varying from one to twelve (see computational details, Table S1 and Fig. 1 and Fig. S1, ESI†). These were the best performing models exhibiting  $m_j = |\pm 9/2\rangle$  or  $|\pm 7/2\rangle$  as their ground state with very low QTM for the given coordination number, which were chosen among a much larger set of models that were screened (forty-two models, see Fig. 1, Fig. S1–S40 and Table S1–S43 in ESI†). Furthermore, calculations were performed on the reported fifteen U(III) complexes that have closer similarity to the models presented to assess and understand various factors that influence the magnetic anisotropy to offer design principles for actinide-based magnets.

Our calculations on various models yield almost pure ( $\geq 90\%$ )  $m_j = |\pm 9/2\rangle$  (Fig. 1 and Table S1, ESI†) as the ground state for one, two, four (tetrahedral), five (trigonal bipyramidal and square pyramidal), six (octahedral), seven (pentagonal bipyramidal), and eight (square antiprismatic) coordinated models and a dominant (*ca.* 70%)  $m_j = |\pm 9/2\rangle$  in one of the twelve coordinate icosahedron models.<sup>8</sup> Furthermore, almost pure  $m_j = |\pm 7/2\rangle$  was stabilised for ten (bicapped square

Department of Chemistry, Indian Institute of Technology Bombay, Powai, Mumbai, 400076, India. E-mail: [rajaraman@chem.iitb.ac.in](mailto:rajaraman@chem.iitb.ac.in); Tel: +91-22-2576-7183

† Electronic supplementary information (ESI) available: Supporting information contains SO states, Tables and the optimized geometries. See DOI: <https://doi.org/10.1039/d2cc01356h>

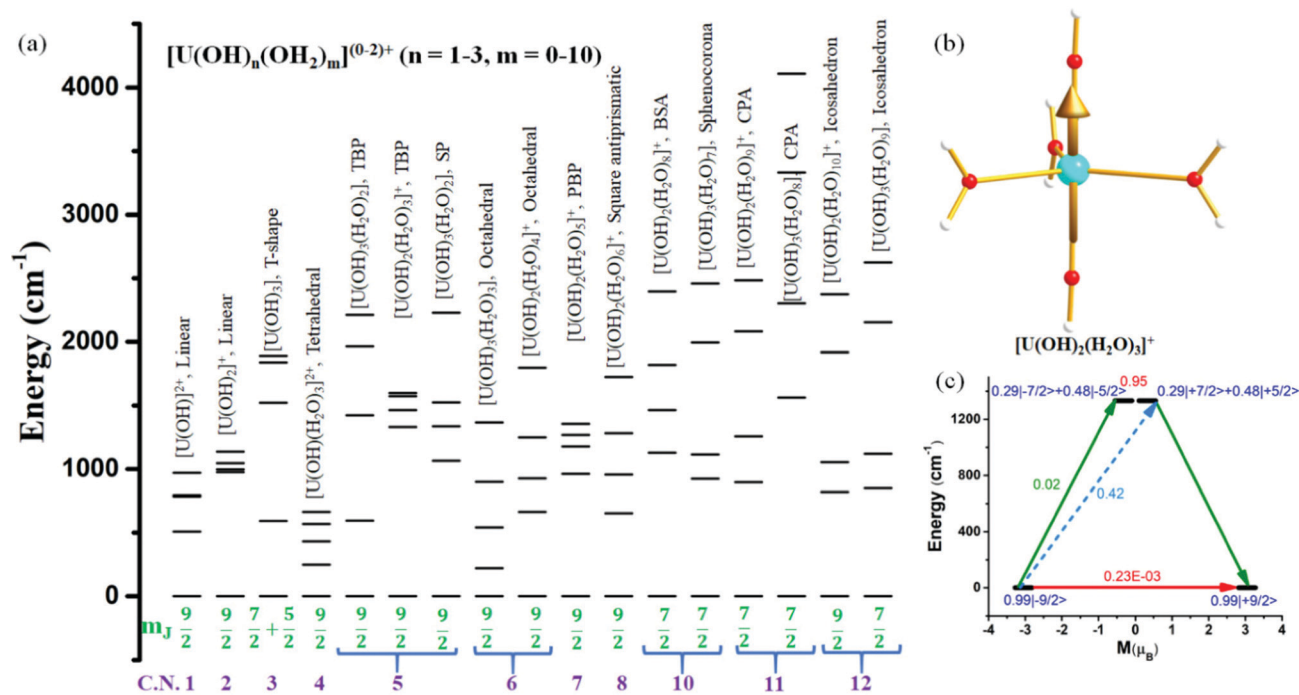


**Fig. 1** (a) The energy of the five KDs generated from  $J = 9/2$  manifold of 17 hypothetical  $[\text{U}(\text{OH})_n(\text{OH}_2)_m]^{(0-2)+}$  ( $n = 1-3, m = 0-10$ ) model complexes estimated from *ab initio* calculations. The dominant  $m_J$  ground state for each coordination number is given at the bottom. Here TBP, SP, PBP, BSA and CPA denote the trigonal bipyramidal, square pyramidal, pentagonal bipyramidal, bicapped square antiprism and capped pentagonal antiprism geometries, respectively. (b) The geometry along with the  $g_{zz}$  axis of KD1 and (c) the corresponding magnetisation relaxation mechanism of the  $[\text{U}(\text{OH})_2(\text{H}_2\text{O})_3]^{2+}$  model. Colour code: U-cyan, O-red, and H-white. The red arrows indicate the QTM and TA-QTM *via* ground and higher excited KD, respectively. The cyan colour arrow represents the Orbach process. The olive arrows denote the most probable pathway to relaxation. The blue number indicates the  $m_J$  composition ( $J = 9/2$ ) of a KD.

antiprismatic) coordinated models and a dominant  $m_J = |\pm 7/2\rangle$  in eleven coordinated (pentagonal antiprismatic) and twelve coordinated (icosahedron, model 2) models. Finally, a combination of  $m_J = |\pm 5/2\rangle$  and  $|\pm 7/2\rangle$  were found to be stabilised in three (T-shape) coordinate models. The  $g_{zz}$  axes of the KD1 in all these models are oriented along the highest order symmetry axis (particularly along with the HO-U-OH bond) to minimise the electrostatic repulsion with the ground state oblate electron density (Fig. S1-S40, ESI<sup>†</sup>). There are two approaches to compute the blocking barrier ( $U_{\text{cal}}$ ) in a SIM; (i) from the energy of the excited KD that possesses large TA-QTM ( $> 10^{-1} \mu_B$ ) or a large deviation ( $> 8^\circ$ ) of the main magnetic axis with the ground state,<sup>9</sup> and (ii) from the sum of the contributions of all KDs within some theoretical models.<sup>8b,10</sup> In our study, we have computed the  $U_{\text{cal}}$  using the first approach. Here, the magnetisation relaxation of all the models occurs *via* the first excited KD except in the three coordinated T-shape models, which relax *via* the second excited KD (Fig. S1-S40, ESI<sup>†</sup>). The computed blocking barrier ( $U_{\text{cal}}$ ) of the models is found to be very large in the range of  $1000 \text{ cm}^{-1}$  for most of the models and  $> 1500 \text{ cm}^{-1}$  for some models (T-shaped, pentagonal antiprism, see Table S1, ESI<sup>†</sup>). Furthermore, the computed  $U_{\text{cal}}$  values inherently assume that relaxation occurs only *via* the Orbach process and if other relaxation processes are operational, this is likely to reduce the estimated/predicted barrier heights.

The best geometry and coordination that yield large  $U_{\text{cal}}$  values were then chosen as a prototype to search on the Cambridge structural database. The X-ray structures that mimic these fictitious models were then chosen further for our study. If suitable uranium complexes were not reported, the search was extended to cover lanthanide/transition metal complexes possessing such geometry and coordination number. For the two-coordinate model, the  $U_{\text{cal}}$  value was estimated to be  $976 \text{ cm}^{-1}$ , and our CCDC search yielded several such examples with lanthanides.<sup>11</sup> Among these  $[\text{U}\{\text{N}(\text{H})\text{Ar}^\#_2\}_2]^{2+}$  (**1**,  $\text{Ar}^\# = \text{C}_6\text{H}_3-2,6-(\text{C}_6\text{H}_2-2,4,6-\text{Me}_3)_2$ ) was modelled by replacing Ln(III) with U(III) followed by geometry optimisation at the DFT level (see computational details, also see Appendix S1 in ESI<sup>†</sup>).<sup>11d</sup> The *ab initio* calculation on **1** confirms a very large blocking barrier of  $962.3 \text{ cm}^{-1}$  with  $m_J = |\pm 9/2\rangle$  as the ground state (Fig. 2a and b, Table S44, ESI<sup>†</sup>), suggesting a potential synthetic target for U(III) SIMs. In coordination number three, two field-induced SIMs have been studied by Mills and co-workers. One of them ( $[\text{U}\{\text{N}(\text{SiMe}_2\text{Bu})_2\}_3]$ , **2**) resides in a trigonal planar geometry and the other ( $[\text{U}\{\text{N}(\text{SiMe}_3)_2\}_3]$ , **3**) in a trigonal pyramidal geometry.<sup>12</sup> The stabilisation of  $m_J = |\pm 1/2\rangle$  as the ground state leads to a substantial QTM in both the complexes (Fig. S41 and S42, ESI<sup>†</sup>).<sup>13</sup> However, the T-shape model yielded a  $U_{\text{cal}}$  value of  $1521 \text{ cm}^{-1}$ . To make this model viable, in our earlier study, we have shown that two T-shape complexes

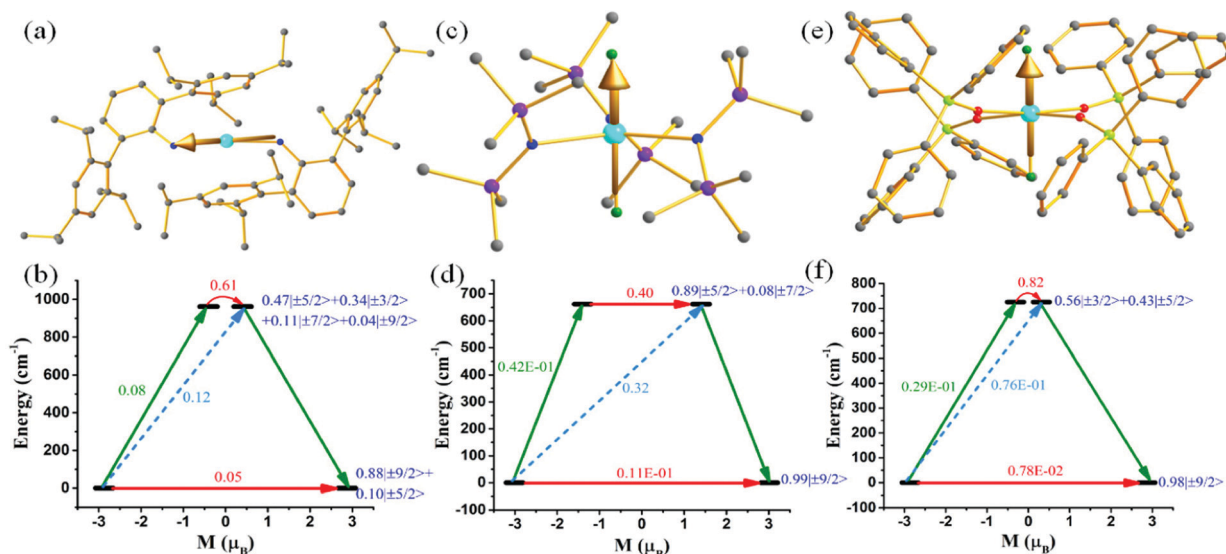


Fig. 2 The  $g_{zz}$  axis of KD1 for (a) **1**, (c) **8F** and (e) **15F**. Colour code: U-cyan, Si- purple, P-light green, F-green, O-red, N-blue, and C-grey. Hydrogens are omitted for clarity. The mechanism of magnetisation relaxation of (b) **1**, (d) **8F** and (f) **15F**. See Fig. 1 for colour description.

([U(NSi<sup>i</sup>Pr<sub>2</sub>)<sub>2</sub>(I)] (**4**) and [U(NHAR<sup>i</sup>Pr<sub>6</sub>)<sub>2</sub>I] (**5**)) are capable of producing large  $U_{\text{cal}}$  values ( $> 900 \text{ cm}^{-1}$ ) which makes them a best-suited target for three-coordinate U(III) SIMs (Fig. S43 and S44, ESI<sup>†</sup>).<sup>13,14</sup>

In four coordination, two tetrahedral SIMs; [U(OSi(O<sup>t</sup>Bu)<sub>3</sub>)<sub>4</sub>]<sup>-</sup> (**6**) and [U(N(SiMe<sub>3</sub>)<sub>2</sub>)<sub>4</sub>]<sup>-</sup> (**7**) have been studied by Mazzanti and co-workers.<sup>15</sup> Our *ab initio* calculations reveal significant QTM in the ground KD originating from the substantial mixing of  $m_j = |\pm 7/2\rangle$  with other states. This is consistent with the experiments yielding very small barrier heights ( $U_{\text{eff}} = 16\text{--}18 \text{ cm}^{-1}$ ; see Fig. S45, S46 and Tables S45, S46, ESI<sup>†</sup>). For further improvement, a tetrahedral fictitious [U(OH)(H<sub>2</sub>O)<sub>3</sub>]<sup>2+</sup> model was carved out (see Fig. 1 and Table S1, ESI<sup>†</sup>) from **6**. As this model has asymmetry in the coordination donor (-OH vs. H<sub>2</sub>O), this generates moderate anisotropy and less QTM with an estimated  $U_{\text{cal}}$  of  $248 \text{ cm}^{-1}$ , and this is perhaps the best model that can be targeted for a tetrahedral U(III) SIM.

As the *ab initio* calculations on the trigonal bipyramidal [U(OH)<sub>2</sub>(H<sub>2</sub>O)<sub>3</sub>]<sup>+</sup> model show a very large  $U_{\text{cal}}$  value, we look at potential candidates in the CCDC. Many U(III) complexes fit these criteria, but the magnetic characterisations were absent.<sup>16</sup> Among these, we have chosen the [UN<sup>\*</sup><sub>3</sub>(CN)<sub>2</sub>]<sup>+</sup> (**8**, N<sup>\*</sup> = N(SiMe<sub>3</sub>)<sub>2</sub>)<sup>16a,17</sup> complex, which has both strong axial and equatorial ligands and hence significant anisotropy was absent (see Fig. S47 and Table S47 in ESI<sup>†</sup>). To improve this further, the -CN groups in **8** were replaced by -F generating a [UN<sup>\*</sup><sub>3</sub>F<sub>2</sub>] (**8F**, see Fig. S48 and Table S48 in ESI<sup>†</sup>) model. This has  $m_j = |\pm 9/2\rangle$  ground state with a very low QTM and a substantial  $U_{\text{cal}}$  value of  $662 \text{ cm}^{-1}$  (Fig. 2c and d), opening up a possibility to obtain decent U(III) SIMs in this class.

In six coordination, we have chosen several U(III) SIMs that were reported in the literature, namely [(U(Bp<sup>Me</sup>)<sub>3</sub>)] (**9**),<sup>6e</sup> [U(Bc<sup>Me</sup>)<sub>3</sub>] (**10**),<sup>6e</sup> [U(Ph<sub>2</sub>BPz<sub>2</sub>)<sub>3</sub>] (**11**),<sup>18</sup> [U(H<sub>2</sub>BPz<sub>2</sub>)<sub>3</sub>] (**12**),<sup>19</sup> [U(Tp<sup>Me2</sup>)<sub>2</sub>]<sup>+</sup> (**13**)<sup>6d</sup> and [U(BIPM<sup>TMS</sup>)(I)<sub>2</sub>(THF)] (**14**),<sup>12b</sup> mostly with pyrazolylborate-based ligands (see Fig. S49–S54,

ESI<sup>†</sup>).<sup>6e,12b,18,19</sup> The U(III) ion in these SIMs possesses a trigonal prismatic geometry ( $D_{3h}$  symmetry) except in **14**, where the U(III) ion has a distorted  $C_s$  symmetry. The *ab initio* calculations on these complexes reveal a significant QTM in the ground state (dominant combination from  $m_j = |\pm 5/2\rangle$  and  $|\pm 7/2\rangle$ ), which hinders them from attaining a large blocking barrier (the  $U_{\text{eff}}$  values of these complexes lie in the range of  $0\text{--}22 \text{ cm}^{-1}$ , Fig. S49–S54 and Tables S49–S52, ESI<sup>†</sup>).<sup>20</sup> As our model [U(OH)<sub>2</sub>(H<sub>2</sub>O)<sub>4</sub>]<sup>+</sup> yields a very large  $U_{\text{cal}}$  value ( $663 \text{ cm}^{-1}$ ) due to the presence of asymmetric donor ligands, a search in the CCDC yields the [UI<sub>2</sub>(OPPh<sub>3</sub>)<sub>4</sub>][I] (**15**, Fig. 2, Fig. S55 and Table S53, ESI<sup>†</sup>)<sup>21</sup> complex meeting the search criteria. For this complex, due to the weaker U–I bond, the SIM characteristics were only marginal (see Fig. S55 and Table S53, ESI<sup>†</sup>). However upon substituting the -I by -F, another model [UF<sub>2</sub>(OPPh<sub>3</sub>)<sub>4</sub>] (**15F**, see Fig. 2e and f) is constructed, which has negligible QTM at the ground state and resulted in a very large  $U_{\text{cal}}$  value of  $725 \text{ cm}^{-1}$  (see Table S54 in ESI<sup>†</sup>). Such models, if targeted for six coordination, could unveil well-performing U(III) SIMs.

In seven coordination, two U(III) SIMs, [UI<sub>3</sub>(THF)<sub>4</sub>] (**16**) and [U(Tp<sup>Me2</sup>)<sub>2</sub>I] (**17**) with distorted pentagonal bipyramidal geometries (PBP) have been studied.<sup>6b,12b</sup> The calculations on both of them reveal a large mixing of  $m_j = |\pm 9/2\rangle$  with other states (Fig. S56–S57 and Tables S55, S56, ESI<sup>†</sup>) and explain the origin of the tiny  $U_{\text{eff}}$  in **16–17** ( $12.8\text{--}21 \text{ cm}^{-1}$ ). Among several models studied, a pentagonal bipyramidal model [U(OH)<sub>2</sub>(H<sub>2</sub>O)<sub>5</sub>]<sup>+</sup> has been found to possess significant magnetic anisotropy (Fig. 1 and Table S1, ESI<sup>†</sup>). As pseudo  $D_{5h}$  complexes containing lanthanides have a similar coordination environment, one such complex reported and studied by us earlier [L<sub>2</sub>U(H<sub>2</sub>O)<sub>5</sub>][I]3L<sub>2</sub>(H<sub>2</sub>O)] (**18**) reveals a moderate  $U_{\text{cal}}$  value of  $328 \text{ cm}^{-1}$  with  $m_j = |\pm 9/2\rangle$  as the ground state (Fig. S58, ESI<sup>†</sup>).<sup>22</sup>

In eight coordination, two U(III) SIMs [U(Tp<sup>Me2</sup>)<sub>2</sub>(bipy)]<sup>+</sup> (**19**) and [U(Tp<sup>Me2</sup>)<sub>2</sub>(bipy)] (**20**) with dodecahedron geometries have been studied.<sup>23</sup> The *ab initio* calculations on **19** reveal a large

ground state transverse anisotropy due to the substantial mixing between  $m_l$  states (Fig. S59 and Table S57, ESI<sup>†</sup>) and explain the origin of small  $U_{\text{eff}}$  ( $18\text{--}23\text{ cm}^{-1}$ ) in these complexes.<sup>6b</sup> While a square antiprism model  $[\text{U}(\text{OH})_2(\text{OH}_2)_6]^+$  yields an attractive barrier height ( $654\text{ cm}^{-1}$ ), a structurally similar  $[\text{U}_3(\text{Me}_4\text{phen})_2(\text{py})]$  (21)<sup>24</sup> reveals significant QTM in the ground state due to the absence of strong axial ligands (Table S58 and Fig. S60, ESI<sup>†</sup>). Various attempted models for nine coordination geometry did not yield attractive  $U_{\text{cal}}$  values and our calculations on the reported tricapped trigonal prismatic U(III) complex<sup>6c</sup> ( $[\text{UTp}_3]$  (22), Fig. S61, ESI<sup>†</sup>) having nine coordination yield strong QTM at the ground state consistent with the experimental  $U_{\text{eff}}$  of  $3.81\text{ cm}^{-1}$  reported.<sup>22</sup>

In 10–12 coordination, bicapped square antiprism ( $[\text{U}(\text{OH})_2(\text{OH}_2)_8]^+$ ), sphenocorona ( $[\text{U}(\text{OH})_3(\text{OH}_2)_7]$ ), two capped pentagonal antiprism ( $[\text{U}(\text{OH})_2(\text{OH}_2)_9]^+$  and  $[\text{U}(\text{OH})_3(\text{OH}_2)_8]$ ) and the icosahedron ( $[\text{U}(\text{OH})_2(\text{OH}_2)_{10}]^+$  and  $[\text{U}(\text{OH})_3(\text{OH}_2)_9]$ ) models were found to yield very attractive  $U_{\text{cal}}$  values in the range from 900 to  $1500\text{ cm}^{-1}$ . Only for ten coordination, a suitable experimental structure is found. The  $[\text{U}(\text{OTf})_2(\text{phen})_4]^+$  (23)<sup>21</sup> complex has a bicapped square antiprism geometry, but calculations reveal poor SIM characteristics due to very weak axial ligands (OTf in X-ray vs.  $-\text{OH}$  in models) and stronger equatorial ligands.

To summarise, our extensive theoretical search for high blocking barrier U(III) SIMs with coordination numbers varying from 1 to 12 yielded several synthetic targets with a barrier height of more than  $1000\text{ cm}^{-1}$  – a value yet to be witnessed for any actinide SIMs. However, as many targets studied are based on reported X-ray structures, this study will likely unveil a new generation of U(III)-based SIMs with attractive blocking barriers.

S. D. would like to thank UGC for a fellowship. G. R. would like to thank CSIR (01(2980)/19/EMR-II) for funding. Both the authors thank Dr Thayalan Rajeshkumar for helpful suggestions in the calculations.

## Conflicts of interest

There are no conflicts to declare.

## References

- (a) S. G. McAdams, A.-M. Ariciu, A. K. Kostopoulos, J. P. Walsh and F. Tuna, *Coord. Chem. Rev.*, 2017, **346**, 216–239; (b) S. T. Liddle and J. van Slageren, *Chem. Soc. Rev.*, 2015, **44**, 6655–6669.
- Y. S. Ding, T. Han, Y. Q. Zhai, D. Reta, N. F. Chilton, R. E. Winpenny and Y. Z. Zheng, *Chem. – Eur. J.*, 2020, **26**, 5893–5902.
- H. Liu, J. Li and B. Yin, *Phys. Chem. Chem. Phys.*, 2022, DOI: [10.1039/D2CP00776B](https://doi.org/10.1039/D2CP00776B).
- (a) F.-S. Guo, B. M. Day, Y.-C. Chen, M.-L. Tong, A. Mansikkamäki and R. A. Layfield, *Science*, 2018, **362**, 1400–1403; (b) C. A.-P. Goodwin, F. Ortu, D. Reta, N. F. Chilton and D. P. Mills, *Nature*, 2017, **548**, 439–442.
- D. Reta, J. G. Kragoskow and N. F. Chilton, *J. Am. Chem. Soc.*, 2021, **143**, 5943–5950.
- (a) J. J. Le Roy, S. I. Gorelsky, I. Korobkov and M. Murugesu, *Organometallics*, 2015, **34**, 1415–1418; (b) J. T. Coutinho, M. A. Antunes, L. C. Pereira, H. Bolvin, J. Marcalo, M. Mazzanti and M. Almeida, *Dalton Trans.*, 2012, **41**, 13568–13571; (c) J. D. Rinehart and J. R. Long, *Dalton Trans.*, 2012, **41**, 13572–13574; (d) M. A. Antunes, I. C. Santos, H. Bolvin, L. C. Pereira, M. Mazzanti, J. Marcalo and M. Almeida, *Dalton Trans.*, 2013, **42**, 8861–8867; (e) K. R. Meihaus, S. G. Minasian, W. W. Lukens Jr, S. A. Kozimor, D. K. Shuh, T. Tyliczszak and J. R. Long, *J. Am. Chem. Soc.*, 2014, **136**, 6056–6068; (f) C. Apostolidis, A. Kovács, O. Walter, E. Colineau, J. C. Griveau, A. Morgenstern, J. Rebizant, R. Caciuffo, P. J. Panak and T. Rabung, *Chemistry*, 2020, **26**, 11293.
- (a) J. D. Rinehart and J. R. Long, *Chem. Sci.*, 2011, **2**, 2078–2085; (b) S. K. Singh, T. Gupta and G. Rajaraman, *Inorg. Chem.*, 2014, **53**, 10835–10845.
- (a) L. Ungur and L. F. Chibotaru, *Inorg. Chem.*, 2016, **55**, 10043–10056; (b) N. F. Chilton, *Inorg. Chem.*, 2015, **54**, 2097–2099.
- (a) L. Ungur, J. J. Le Roy, I. Korobkov, M. Murugesu and L. F. Chibotaru, *Angew. Chem., Int. Ed.*, 2014, **126**, 4502–4506; (b) J. Liu, Y.-C. Chen, J.-L. Liu, V. Vieru, L. Ungur, J.-H. Jia, L. F. Chibotaru, Y. Lan, W. Wernsdorfer and S. Gao, *J. Am. Chem. Soc.*, 2016, **138**, 5441–5450.
- (a) N. F. Chilton, C. A. Goodwin, D. P. Mills and R. E. Winpenny, *ChemComm*, 2015, **51**, 101–103; (b) D. Aravena, *J. Phys. Chem. Lett.*, 2018, **9**, 5327–5333; (c) B. Yin and C.-C. Li, *Phys. Chem. Chem. Phys.*, 2020, **22**, 9923–9933; (d) A. Castro-Alvarez, Y. Gil, L. Llanos and D. Aravena, *Inorg. Chem. Front.*, 2020, **7**, 2478–2486.
- (a) N. F. Chilton, C. A. Goodwin, D. P. Mills and R. E. Winpenny, *Chem. Commun.*, 2015, **51**, 101–103; (b) H. M. Nicholas, M. Vonci, C. A.-P. Goodwin, S. W. Loo, S. R. Murphy, D. Cassim, R. E.-P. Winpenny, E. J.-L. McInnes, N. F. Chilton and D. P. Mills, *Chem. Sci.*, 2019, **10**, 10493–10502; (c) C. A. Goodwin, N. F. Chilton, G. F. Vettese, E. Moreno Pineda, I. F. Crowe, J. W. Ziller, R. E. Winpenny, W. J. Evans and D. P. Mills, *Inorg. Chem.*, 2016, **55**, 10057–10067; (d) W. A. Merrill, T. A. Stich, M. Brynda, G. J. Yeagle, J. C. Fettinger, R. De Hont, W. M. Reiff, C. E. Schulz, R. D. Britt and P. P. Power, *J. Am. Chem. Soc.*, 2009, **131**, 12693–12702.
- (a) C. A. Goodwin, F. Tuna, E. J. McInnes, S. T. Liddle, J. McMaster, I. J. Vitorica-Yrezabal and D. P. Mills, *Chem. – Eur. J.*, 2014, **20**, 14579–14583; (b) F. Moro, D. P. Mills, S. T. Liddle and J. van Slageren, *Angew. Chem., Int. Ed.*, 2013, **125**, 3514–3517.
- S. Dey and G. Rajaraman, *Inorg. Chem.*, 2022, **61**, 1831–1842.
- C. A.-P. Goodwin, F. Tuna, E. J.-L. McInnes and D. P. Mills, *Eur. J. Inorg. Chem.*, 2018, 2356–2362.
- L. C. Pereira, C.-m Camp, J. T. Coutinho, L. Chatelain, P. Maldivi, M. Almeida and M. Mazzanti, *Inorg. Chem.*, 2014, **53**, 11809–11811.
- (a) A. Hervé, Y. Bouzidi, J.-C. Berthet, L. Belkhiri, P. Thuéry, A. Bouekkine and M. Ephritikhine, *Inorg. Chem.*, 2015, **54**, 2474–2490; (b) P. L. Arnold, L. Puig-Urrea, J. A. Wells, D. Yuan, F. L. Cruickshank and R. D. Young, *Dalton Trans.*, 2019, **48**, 4894–4905.
- A. Hervé, Y. Bouzidi, J.-C. Berthet, L. Belkhiri, P. Thuéry, A. Bouekkine and M. Ephritikhine, *Inorg. Chem.*, 2014, **53**, 6995–7013.
- J. D. Rinehart and J. R. Long, *J. Am. Chem. Soc.*, 2009, **131**, 12558–12559.
- J. D. Rinehart, K. R. Meihaus and J. R. Long, *J. Am. Chem. Soc.*, 2010, **132**, 7572–7573.
- (a) S. Dey, G. Velmurugan and G. Rajaraman, *Dalton Trans.*, 2019, **48**, 8976–8988; (b) M. Spivak, K. D. Vogiatzis, C. J. Cramer, C. D. Graaf and L. Gagliardi, *J. Phys. Chem. A*, 2017, **121**, 1726–1733; (c) M. A. Antunes, I. C. Santos, H. Bolvin, L. C. Pereira, M. Mazzanti, J. Marcalo and M. Almeida, *Dalton Trans.*, 2013, **42**, 8861–8867; (d) J. J. Baldoví, S. Cardona-Serra, J. M. Clemente-Juan, E. Coronado and A. Gaita-Ariño, *Chem. Sci.*, 2013, **4**, 938–946.
- J.-C. Berthet, M. Nierlich and M. Ephritikhine, *Polyhedron*, 2003, **22**, 3475–3482.
- S. Dey and G. Rajaraman, *J. Chem. Sci.*, 2019, **131**, 124.
- J. T. Coutinho, M. A. Antunes, L. C. Pereira, J. Marcalo and M. Almeida, *Chem. Commun.*, 2014, **50**, 10262–10264.
- J.-C. Berthet, J.-M. Onno, F. Gupta, C. Rivière, P. Thuéry, M. Nierlich, C. Madic and M. Ephritikhine, *Polyhedron*, 2012, **45**, 107–125.